FEBS Letters 571 (2004) 134–140 FEBS 28621

Heterogeneity based on bending of purple membrane containing bacteriorhodopsin

Hamdy I.A. Mostafa

Department of Biophysics, Faculty of Science, Cairo University, 12613 Giza, Egypt

Received 18 May 2004; revised 16 June 2004; accepted 17 June 2004

Available online 6 July 2004

Edited by Richard Marais

Abstract The first and second derivatives of dielectric spectra have evidenced the existence of two interacting states of purple membrane (PM) that respond differently to the intensity of illuminating light providing, this way, underlying consequences to the heterogeneous behavior of bacteriorhodopsin (bR). It is of particular interest to note that the rotational diffusion coefficient of PM has exhibited non-linearity versus light intensity. The explored non-linearity in electrical properties beers, thereby, on changes in PM size. The non-linear variations in PM bending might initiate, in consequence, variations in the dipole moment (permanent and induced) and dc-conductivity of PM patches. Proposal based on PM bending has been introduced to correlate the light intensity effect to the PM lipid environment. Modulation of the global structure of PM and, in turn, its electrical properties by an external perturbation (e.g., light) could be of interest in biotechnological applications based on optoelectronic properties of bR.

Keywords: Actinic light intensity; Purple membrane bending; Heterogeneity; Permittivity; Conductivity

1. Introduction

The purple membrane (PM) of the archaeal *Halobacterium salinarum* is a highly specialized biological structure. The asymmetry is one of its inherent characteristics [1]. Its bending seems to be another inherent property that is expected to have underlying consequences in different behaviors of bacteriorhodopsin (bR). The bR molecules (together with lipids) are organized as trimers forming the two-dimensional hexagonal lattice of PM. The spaces between bR molecules and those outside and inside the bR trimers are filled with particular lipid molecules in a particular asymmetric distribution on both sides of PM [2,3]. The ratio of protein to lipid in PM is 75–25% by weight (i.e., 10 lipid molecules per one bR molecule). The precise location of lipids in PM crystal structure remains unresolved and the location of some of them was tentatively determined. These PM native lipids have proved to be of potential role in maintaining such PM crystal structure, insomuch that if they were replaced with other types of lipids, disruption of the PM crystal would be the result. Such high specific and significant interactions between lipid and bR would, in consequence, underlie the curvature of such rigid PM. Phytanyl chains of PM lipids allow their headgroup to be located in larger spacing than with saturated unbranched alkyl ones. This unique property may, in addition, participate to enhance the bending. Several factors (e.g., pH [4], temperature [5], and lipid environment [6,7]) were investigated to cause bending of PM. In the second place, the same factors were found to affect the bR–lipid contacts. This would correlate the bending of PM to the role of its lipid. Also the same factors were found to affect (or modulate) the photocycle of bR. Since the intensity of exciting light has long been known to regulate the bR photocycle [8,9], it would be expected that light intensity causes bending of PM. The light intensity effect is, however, quantified by the ratio (M_f/M_s) present in a single turnover, where M_f and M_s are the amplitudes of fast M (2 ms) and slow M (6 ms) intermediates, respectively, in the bR photocycle. The mole fraction of M_f, at neutral pH, varies from 0.8 at low to 0.5 (or less) at high light intensity [9]. At low flash power, the M_f predominates directing the photocycle to the regenerated ground state of bR through the pathway of O-intermediate formation, while at high flash power M_f is getting slower to become M_s (or replaced with other slower M forms) directing the photocycle directly to bR bypassing the O-shunt. The merits of parallel independent photocycles seem to be evident, even though the origin underlying this behavior was subjected to debate [9–11], i.e., whether it arises from cooperativity or/and heterogeneity. Being bR is trimeric in PM makes sense that cooperativity should not be excluded. Such type of cooperative mode should be in view of the PM lattice (i.e., between bR trimers, not within one trimer unit). The trimers structure remained without loss (only the lattice was damaged) [12] after subjecting PMs to brief exposure (1 min) of less than 0.2% of Triton X-100. These trimers showed photocycle independent of the light intensity, similarly like the case of bR monomers [12,13]. This brief exposure was enough to eliminate both M_f and O intermediates from the bR photocycle inducing the formation of much slower M_s, and enough to make the actinic light to cease modulating the photocycle.

The bR photocycle kinetics is, however, outside the focus of this paper. Directing the studies, instead, toward the global structure of PM fragments may clarify such unresolved behaviors, than the local fine structure. In a recent work [14], it has been showed that PMs are of different global structures in light and dark-adapted states. An interest of the present work is, therefore, aimed at exploring the global structure of PM at different intensities of the illuminating light. The current results have showed that there have been two interacting states of PM that respond differently to the photon density. The results have been exploited to explain that there has been one state (assigned to M_f) predominating at low intensity, while

E-mail address: hamszil@yahoo.com (H.I.A. Mostafa).

0014-5793/$22.00
doi:10.1016/j.febslet.2004.06.066

the other state (assigned to M_s) is predominating at high light intensity. The intention of studying the global structure versus light intensity has, however, been ensued from the criterion that both the transmittance of bR was increased [12] and the light scattering of PM suspension was decreased, upon the brief exposure of PM to 0.05% Triton X-100. Interestingly, the BR photocycle in Triton-treated PM could regain its normal behavior by reconstituting it with native PM lipids [15]. In accordance to the crucial role of lipids in regulating the bR photocycle, a proposal based on PM bending has been introduced, in the present work, to correlate the light intensity to lipid environment effect.

2. Materials and methods

Cells of *H. salinarum* Strain S-9 were grown and their PMs were prepared according to well-established standard method [16]. The concentration of PM was adjusted, on the basis of an extinction coefficient of 63 000 cm^{-1} M^{-1}, to 4 μM in distilled water with very little adjustment to pH 6.6 with the addition of HCl so as to keep it as low ionic strength solution. The measurement of the dielectric data was carried out by measuring the parallel capacitance (C) and resistance (R) of bR sample solution. The cell employed in the measurements was made of platinum black and whose cell constant was 0.0265 m^{-1}. The cell constant (K) was determined using methanol solution and kept as a global constant during the iterative fitting of the dielectric data employing software in genetic algorithm. The measurement was taken, over the frequency range from 20 Hz to 1 MHz, by employing ChenHwa 1069 LCZ meter and LCR-bridge (Hioki 3532 LCR Hi-Tester) interfaced to a computer. It should be noted that only few points from 20 to 40 Hz were recorded via the ChenHwa 1069 meter. The sample connection was carried out through a Test Fixture (Hioki 9261) where the sinusoidal electric field applied to the electrode was 1 V/cm. The data (100 points) were recorded at room temperature (20 °C). The measurement was repeated at different light intensities incident on bR sample. The maximum light intensity was considered as 600 mW/cm^2, while the minimum one as 3 mW/cm^2. Starting the dielectric spectrum measurements with zero light intensity (i.e., dark adapted state of bR with 13-*cis*, 15-*syn* retinal isomer) was avoided in order to have a bR sample of the same chromophore configuration (i.e., light adapted bR with 13-*trans*, 15-*anti* retinal isomer). This has to be considered into account because both states of bR (dark and light adapted) have been observed to have quite different electrical parameters [14]. Therefore, the PM containing bR was, firstly, dark adapted for 3 days (at pH 6.6 and at 25 °C) and then light adapted with the minimum light intensity. The dielectric spectra were started, at that intensity, to be recorded. The subsequent dielectric measurements were carried out at increasing levels of light intensity till its maximum value. The measuring electrode set-up was made appropriate so as to minimize the impedance of the electrode polarization [17]. Even the residual of electrode polarization impedance was considered in the iterations that are carried out to fit the experimental data. The light intensity was changed via changing the electric current supplied to 300-W lamp. A heat filter ($CuSO_4$ solution) was inserted between the illuminating light source and the cell containing bR sample in order to avoid any heating effect.

3. Results

The curves relevant to ac-conductivity keep on displaying significant vertex at about 100 mW/cm^2 for the whole frequency range, whereas less pronounced increases (and sometimes decreases) are observed for the curves relevant to relative permittivity around that value of intensity, as shown in Fig. 1. To be so non-linear implies that they likely impart non-linearity to the electrical parameters of PM. The latter could be deduced using the parameters of the deconvoluted dielectric

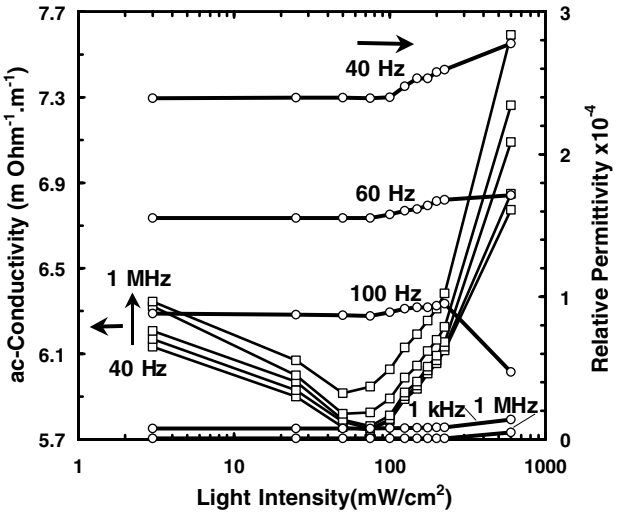

Fig. 1. The intensity dependence of relative permittivity (right) and ac-conductivity (left) at different frequencies. A prominent vertex around 100 mW/cm^2 is shown for ac-conductivity.

dispersions of PM. A genetic algorithm is used to decompose the measured dielectric spectrum of PM into different components whose sum fits well to the measured data points. As an example, Fig. 2 shows the deconvolution of the dielectric spectrum in case of the minimum light intensity (3 mW/cm^2) into three dielectric dispersions, along with their summation. For each deconvoluted dispersion, three types of curves are depicted, i.e., the curves relevant to the relative permittivity (ε'), ac-conductivity (σ_{ac}) and dielectric loss (ε''). The assignment of the three dispersions has already been given in detail, very recently, in a previous measurement [14]. They are around 15 mHz, 20 Hz and 1.4 kHz. The first two are in consequence to the rotation of the whole PM fragment

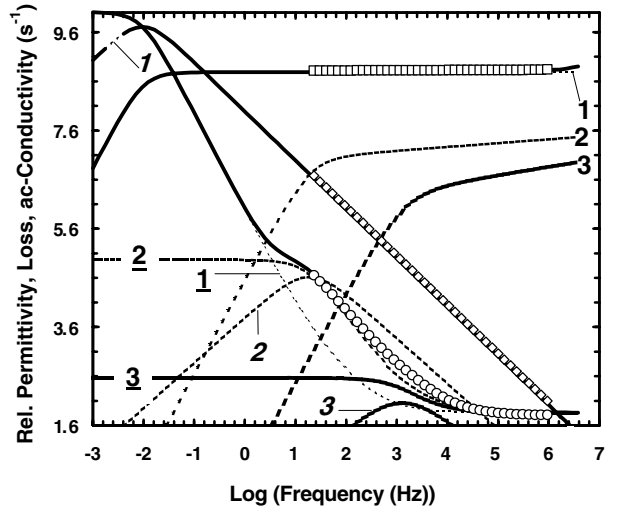

Fig. 2. Deconvolution of the dielectric spectrum of PM, for example at 3 mW/cm^2, into three dispersions. For each one, three dielectric representations are given: relative permittivity (circles), dielectric loss (diamonds), and ac-conductivity (squares in unit of 1/s) on log-scale. Solid lines are due to curve fitting and they are the sum of the three deconvoluted dispersions plus baseline (infinite dielectric constant for relative permittivity, whereas dc-conductivity for ac-conductivity).

around, respectively, its major axis (x) and its minor axis (y), due to the component of permanent dipole moment (μ_x and μ_y) of PM assigned to each axis of revolution. The third one is a consequence to rotation of the whole PM fragment due to its induced dipole moment. In the first two orientations, PM surface is perpendicular to the orienting electric field, whereas PM surface, in the third one, is parallel with the orienting field direction. This was in agreement with earlier electric dichroism studies [18–20]. It should be noted that the optimization of dielectric data has necessitated the introduction of such first dispersion due to the large dielectric loss exhibited by such large fragments like PMs. It was of interest to consider, in addition, such dispersion in accounting the light intensity effect.

The dielectric spectra have been processed in terms of its differential calculus, as the first and/or second derivatives allow spectral changes to be noticeable. These derivative analyses have showed prominent isosbestic points. These points are revealed by the intersection of all traces of $[dE'/d(F)]$; where $F = \log_{10}(f)$ and $E = \log_{10}(\varepsilon')$, as seen in Fig. 3A. The amplitudes of the negative small peak located at 10 Hz (before the point P1) together with its fractional relative to those corresponding amplitudes at, for example, 10 kHz (after P1) are shown at the inset in Fig. 3A. Examining these amplitudes versus the intensity of the light beam was found to explore non-linearity. Likewise representation was made for the second derivative of relative permittivity $[d^2E'/d(F)^2]$ and depicted in Fig. 3B. The amplitude A_1 is positioned at about 15 mHz (i.e., f_{c1} of first dispersion), whereas the amplitudes A_2 and A_3 are, respectively, located at 20 Hz and 1.4 kHz (i.e., f_{c2} and f_{c3} of second and third dispersions, respectively). This was just an interest to show that PM has dielectric spectrum of at least three prominent dispersions as judged by the deconvolution of the experimental native spectra. It should be noticed that there has been a prominent isosbestic point at 3 kHz (call it P2) through which all traces keep on passing, as shown in Fig. 3B. The variations of the amplitudes (A_2 and A_3) of $[d^2E'/d(F)^2]$ against light intensity have declared some non-linearity, as seen in the inset of Fig. 3B.

This feature makes a non-optical technique such dielectric spectroscopy to have a powerful approach in elucidating variations in the global structure and, in turn, in the electrical parameters of PM. The fitted parameters, according to Cole and Cole model [21], of the deconvoluted dispersions were used to evaluate the dipole moment (permanent and induced) and dc-conductivity of PM, in addition to its rotational diffusion coefficient. The latter could be determined from the relaxation time of PM fragment along largest and smallest axes. Dealing with the rotational diffusion coefficient to get a figure about the size of fragments is so fruitful as the former depends on the third power of the hydrodynamic radius. This means that very small variations in the dielectric relaxation time could lead to noticeable variations in size. It is known that the dielectric increment ($\Delta\varepsilon$) of dispersion is proportional to the square of the dipole moment (permanent or induced) along the axis of revolution. All these parameters of PM have so non-linear behavior versus the light intensity as seen in the panels of Fig. 4. It is also interesting to note that all parameters have fairly exhibiting s-shaped behavior with the photon density, except the dc-conductivity. It has rather followed the changes of ac-conductivity against light intensity. The dc-conductivity has plainly exhibited sharp minimum pointed at 100 mW/cm^2, too, as shown in Fig. 5. Determining the permanent dipole moment of PM and its relaxation time is, therefore, of great interest, to follow the changes in the global structure of PM versus light intensity. Each rotational relaxation is, in consequence, due to the component of permanent dipole moment along such axis of revolution. This makes it possible to estimate, for PM, a minor radius of ~0.18 μm (due to ~25 MDebye permanent moment along minor axis) and major radius of ~2 μm (due to ~4 GDebye permanent moment along major axis). These results seem reasonable, as images of PM patches by atomic force microscopy were found to be of irregular shape with lateral dimensions up to 5 μm and constant thickness of 5 nm [22]. Also by atomic force microscopic studies [23] PM patches with a diameter of 1–3 μm were investigated in their native state in buffer solution. Magnetic birefringence studies [24] showed PM of diameter ranging from 0.2 to 2 μm. It was long thought that PM is circular flat disk of

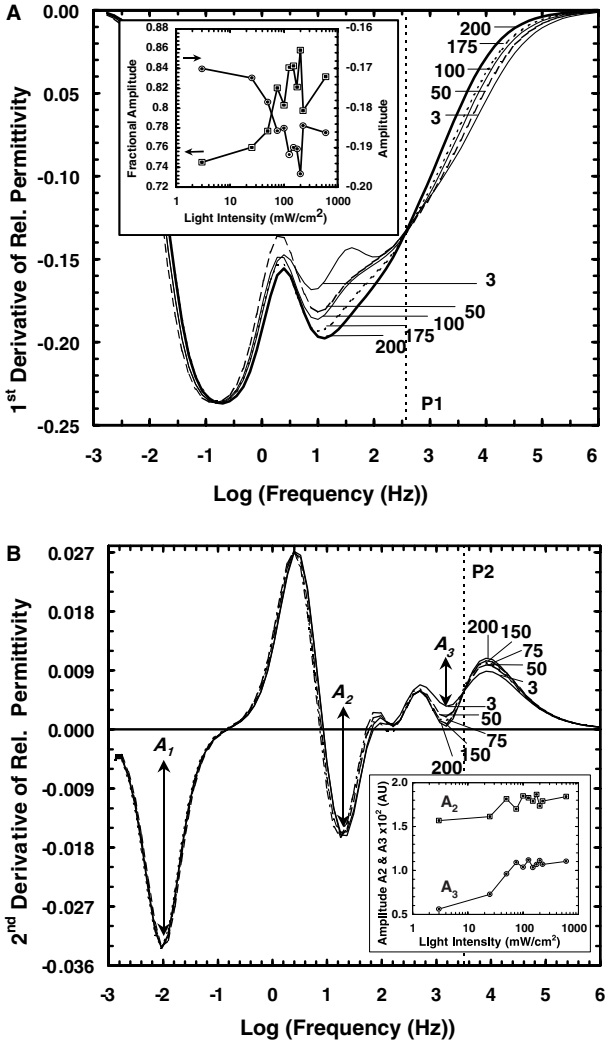

Fig. 3. In (A) the first derivatives of relative permittivity show isosbestic points (e.g., P1). The amplitude at 10 Hz and its fractional $[A_{10\ Hz}/(A_{10\ Hz} + A_{1\ kHz})]$ are shown in the inset. In (B) the second derivatives of relative permittivity show isosbestic points (e.g., P2). The amplitudes A_2 and A_3 versus light intensity are shown in the inset.

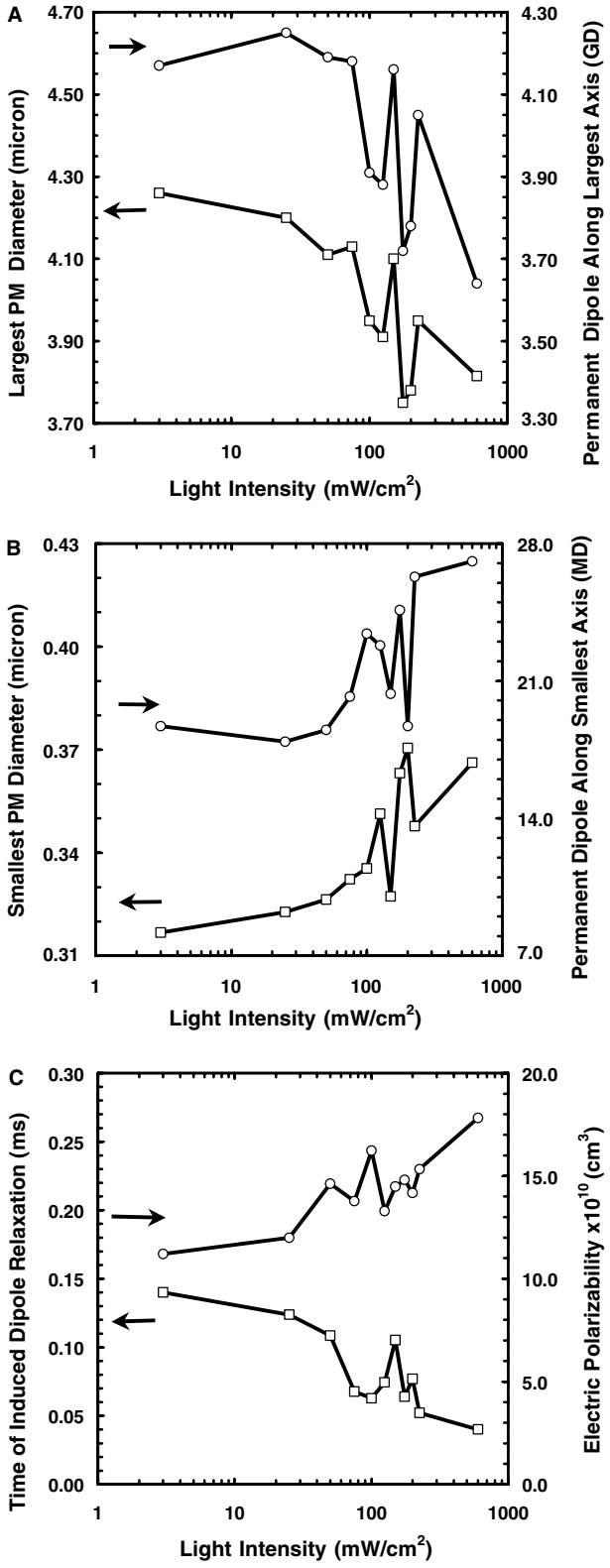

Fig. 4. In (A) parameters of the first dispersion (PM rotation around its large axis). In (B) parameters of the second dispersion (PM rotation around its small axis). In (C) parameters of the third dispersion (PM orientation due to induced dipoles).

1 μm in diameter. This may not be the case for PM, as predicted from the current data. It is, rather, an oval disk of >4 μm long and >0.3 μm wide. This would give an axial ratio very

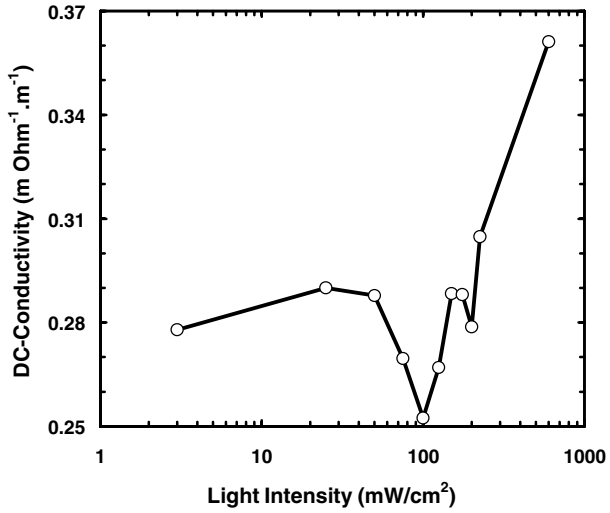

Fig. 5. Variations in dc-conductivity show prominent minimum at 100 mW/cm^2 similar to the vertex shown for the curve relevant to ac-conductivity in Fig. 1.

close to the axial ratio of the *Halobacterium* cell, which is 10–12 μm long and 0.5 μm wide [25]. PM is bent in intact cell toward cytoplasmic (CP) side. This bend is possibly cylindrical (along one axis) not circular (along two axes), as the cell itself represents long cylinder. If one considers that bR represents 80% in the whole membrane of the cell, one can roughly estimate the number of PM per whole surface area of the cell to be at most 4–6 PMs/cell, aligned with their longitudinal axis (x) parallel with the cell's longitudinal axis. The isolated PMs, this way, might possibly show cylindrical bend along one axis at one time and along the other axis at other time depending on the effect of their circumstances (e.g., pH, light intensity, lipid environment). As inferred from the data shown in Figs. 4A and B, PMs seem to bend along its smallest axis at low light intensity, while its largest axis has no (or little) bend. This situation might be reversed at high light intensity to have PMs bending along the largest axis, instead of the smallest one. This could be considered as a criterion of having PM bending that could respond differently with the light intensity (i.e., having two different states of PM). The existence of isosbestic points (like P1 and P2) has to confirm the existence of interacting states of PM each having different parameters for their global structure. PM would, subsequently, bend along the smallest axis (i.e., around the largest axis) at high photon density, whereas the bend, at low photon density, would be along the largest axis (i.e., around the smallest axis). The bending is known to be toward EC at pHs above 5 and toward CP side below pH 5 as judged from light scattering studies [4], whereas at pH 5 PM is more or less flat [19,20]. The current measurements were carried out at near neutral pH. This was an interest to follow the pK_a (6.6) of the light intensity effect [26], where at high alkaline pHs the aforementioned intensity effect becomes more pronounced. The turnover of PM bending from bending state along one axis to bending state along the other axis might, therefore, be correlated to the turnover of M_f and M_s during the late photocycle due to light intensity effect. The transition between the two PM states versus light intensity (I) dependence is located at pI_a of ~100 mW/cm^2 (equivalent to the turnover of M_f and M_s versus pH located at pK_a of ~6.6

[26]). A pI_a of ~100 mW/cm^2 could gain correlative support from studies based on non-linear optical properties of bR. The bR is known to be a sensitive non-linear absorber of light with very low saturation intensity. The non-linear coupling of two beams in a saturable absorber like bR was found to enhance strongly the beams' transmissivity [27]. This non-linear two-beam coupling-induced transparency occurs when two mutually coherent beams traverse bR (saturable absorber). The coupling-induced transparency for the weak and strong beams was observed to display maximum, interestingly, at around 100 mW/cm^2. Studying the global structure of PM at coupling of two beams (weak and strong) would, thereby, be expected to be fruitful. The transmittance for the chemically untreated WT-bR film as a function of exciting beam intensity [28] was found to have a maximum at 100 mW/cm^2. The optical properties of bR to be so non-linear would thus entail, in a correlative sense, that its electrical properties be non-linear, too. The photocurrent and photovoltage in a bR film have, however, showed exponential dependences on the flash power, as reported in recent photovoltaic studies [29].

4. Discussions

The transition between the two states, at weak and strong light, may involve conformational changes, which affects the protein–protein and protein–lipid contacts. Light illumination did cause changes to the surface structure of the bR lattice as reported in atomic force microscopic studies [23] made on PMs adsorbed to mica with their EC side. Thus, such conformational changes and the inter-trimer interactions might partly be induced by the change in surface charges and might be electrostatic in origin. In regard to the light intensity effect, fast and slow Schiff base deprotonation implies, simply, that two different Schiff base environments have to be existed. The phenomenon is known to become pronounced at alkaline pHs [26]. This would be consistent with the proposal that was ruled out in pH studies [30]. This proposal was that the protonated Schiff base has two different sites within the protein; one located near a tyrosine and slowly deprotonates during the photocycle, whereas the other site is near a tyrosinate ion and deprotonates rapidly, meriting, this way, the validity of heterogeneity. Several studies did impart support to the existence of heterogeneity effect. At neutral pH, bR was observed to have two spectroscopically undistinguished forms [31], evidencing the existence of heterogeneous bR populations. Even the binding of all-*trans* retinal to the apo-protein (bacteriorhodopsin) has been raised in view of heterogeneity effects in recent reconstitution studies [32]. All these clues refer to the idea of two different PM populations. The current results do favor the heterogeneity effect, as the analysis of the dielectric spectra could attest to the fact of having two interacting states of PM. The appearance of isosbestic points suggests conversion between two distinct states. Both states might be of different electrical properties depending on the light intensity. Whether the light-induced conformational changes of PM or the preferential selection of light intensity to one of the already present bR populations is the cause of heterogeneity is an open question. Based on the present studies regarding the light intensity effects, one may suggest that the light intensity effects be resulted from photoselection based on pre-existing structural differences in bR populations. In the meanwhile, one could not exclude the possibility of interconversions of the interacting states of bR. This would be indicated from the proposal that correlates the light effect to the lipid effect. The participation of both pre-existing heterogeneity and inducement heterogeneity could gain support from studies [33] dealt with the three-dimensional bacteriorhodopsin crystals harvested from a lipidic cubic phase regarding the dehydration effect, which have revealed the presence of three distinct protein species. In these studies, it has been proposed that the main source of this compositional heterogeneity has ensued from partial dehydration during crystallization and/or room temperature conditions. In the meanwhile, there has been interconversion of the species upon intentional dehydration, which has provided support to its assignment as the cause of heterogeneity. One may interpret the changes in the curvature of PMs [34] as distortions in the protein structure owing to its 75% of the PM as large-scale conformational changes would be expected to cause bending. In the meanwhile, it is difficult to imagine such bending without assuming simultaneous specific protein–lipid interactions having to occur to enhance such bending. Partial delipidation of PM was showed to affect the surface charge and electrical properties of PM [6]. In accordance, a proposal based on PM bending has to be introduced to correlate the light intensity effect to the crucial role of lipid environment, in modulating the bR behavior.

Perturbation of the lipid environment of bR trimers is known to modulate, like the actinic light, the photocycle in microsecond time domain of M-intermediate. The light intensity seems to perturb some undefined PM parameters to modulate the amplitude ratio (M_f/M_s). Particular lipids are, therefore, implicated in the ability of light to modify the bR photocycle. Strangely enough that quite different perturbations (e.g., PM lipid, actinic light, pH) can modulate similar behavior (i.e., modulation of the ratio M_f/M_s). These different perturbations most likely mediate their effect via lipid–bR interactions. The neutral lipid squalene (SQ) and the negatively charged phosphatidylglycerophosphate methyl ester (PGP-Me), along with amino acid centers (Asp36, Asp38, Asp102 and Asp104 in loops on CP side encircling a "ring" around the trimer), are known to have significant role for the light intensity effect. It is well established that an electrically neutral environment (provided by SQ) around negatively charged centers (provided by acidic "ring"), together with the approach of negatively charged lipid (provided by PGP-Me) to that of negatively charged centers, is crucial for the M_f eliciting photocycle [26]. In accordance, bending of PM at strong light would be so in the sense that might allow M_f activity to diminish or disappear, as a consequence of the decreased repulsion between the two entities (PGP-Me and amino acid "ring"). This would be rationalized if the bending would, this way, displace SQ [and in consequence to its carrier (i.e., PGP-Me)], away from the negative ring (acidic amino acids on CP side of the trimer). Both of them (SQ and PGP-Me) act synergistically and both are crucial for the environment of M_f eliciting photocycle. These displacements might increase the space that was assigned to the hydrophobic SQ. Besides its hydrophobicity, specific size of the latter (i.e., fitness of SQ to its assigned space) was observed to be another requirement for the predominance of M_f activity [26]. This would come in consistence with the current results, as inferred from Figs. 4A and B, that PM bends along its largest axis at high light in-

tensity, whereas it bends along its smallest axis at low intensity. Bending along its largest axis (~4 μm) would effectively result in more pronounced diminishing in the M_f activity than along its smallest axis (~0.3 μm). The optical anisotropy changes versus time in immobilized PM during the photocycle at stronger light – that were reported in a photoselection measurements [11] – would, therefore, be consistent to the bending of PM along its large axis at our strong light. Likewise, their report [11] that no optical anisotropy changes occurred at weak light, too, is a further confirmation to the current data that no PM bending along its largest axis has occurred at weak intensity, as inferred from Fig. 4A. The authors in these photoselection studies [11] did agree with the fact that the changes in the dichroic ratio are improbable to be a consequence of tilting of the retinal chromophore. Then, it would be a consequence of PM bending. They, however, favored the photocooperativity effect to interpret their data by assuming that the angular distributions of the late photocycle intermediates are regulated by the angular distribution of the photocycling bR molecules.

The virtue of proposing the effect of lipid environment in accounting for variations of the global structure and, in turn, electrical parameters of PM could be reflected from a light scattering studies [6] that reported changes in the dipole moments (induced and permanent) and the electrokinetic charge of PM upon partial delipidation of PM by Tween 20. For example, a lower polarizability of PM at weak, than at strong, intensity may confirm the requirement of M_f activity to neutral environment of SQ (the only neutral lipid in PM of 10%). Bending-induced dislocation, of both the neutral SQ and the negatively charged PGP-Me, away from the negatively charged ring, might impose certain ion distributions that make the moment of induced dipoles of PM lower, but with slower relaxation time, at weak than at strong intensity, as seen in Fig. 4C. This idea could be supported by the finding that addition of the most hydrophobic alkane (decane) to PM in the range of 0.01–0.2% resulted in conversion of M_s to M_f [26]. Even the neutral solubilizing detergent (Triton X-100), when added in very small amounts (0.01–0.02%) to PM, increased the M_f in WT-PM [12]. It is worth, in these regards, to note that the neutral SQ affected the reprotonation of Schiff base by D96 at the late photocycle [35]. Along with the bending effect, the SQ effect would be correlated to conformational changes resulting in an opening in CP side during photocycle. If so, tilting of the retinal polyene chain out of PM plane would be in consequence to bending. A tilting of about 11 degree [36], during the M decay relative to the ground state light adapted bR, might be consistent to the strong bending (50% decrease in PM size) that has been reported, recently, in electric dichroism studies [34] during M intermediate. Crystallographic studies, indeed, reported lateral motions of ~0.35 nm at the CP side of F-helix, evidently causing an opening of a channel on CP side to allow reprotonation of the retinal [37]. Strikingly similar opening was reported but on EC side by the helices A, B, C and D for the bR mutant D85S. This may, likewise, offer bending based clues for the shunt of M_f eliciting photocycle via O-intermediate at low flash power. The X-ray diffraction structure of O-intermediate is, however, generated by virtue of the crystal D85S mutant only [38]. Further clues from the dc-conductivity of PM signify a feeling of interest about the influence of light intensity on membrane potential, which could modulate the photocycle. The relative amounts of M species during a single turnover of bR are known to be, dramatically, varied with variations of membrane potential. Proton pumping could be regulated by membrane potential [39] under voltage clamp and patch clamp conditions. This would explain changing of the dc-conductivity, as seen in Fig. 5, versus light intensity effect. This regard could help in understanding how bR photocycle kinetics could be so different in consequences to the light intensity effect.

In conclusion, the non-linear bending responses, to a perturbation with a pulse of light intensity, of PM signify an important interest from a biotechnological point of view. It would produce a hypothesis of photomechanical nanostructure based on bR. It remains, anyhow, unclear what the driving force is for the PM bending. The mechanism that couples the PM bending to the modulation with light intensity is also not entirely clear.

References

[1] Zingsheim, H.P., Neugebauer, D.C. and Henderson, R. (1978) J. Mol. Biol. 123, 275–278.
[2] Hendler, R.W. and Dracheva, S. (2001) Biochemistry (Moscow) 66, 1623–1627.
[3] Cartailler, J.-P. and Luecke, H. (2003) Annu. Rev. Biophys. Biomol. Struct. 32, 285–310.
[4] Czégé, J. and Reinisch, L. (1991) Photochem. Photobiol. 54, 923–930.
[5] Shnyrov, V.L., Tarakhovskii, Y.S. and Borovyagin, V.L. (1981) Bioorganich. Khimiya. 7, 1054–1059.
[6] Taneva, S.G., Dobrikova, A., Petkanchin, I.B. and Goni, F.M. (1995) Bioelectrochem. Bioenerg. 38, 111–115.
[7] Denkov, N.D., Yoshimura, H., Kouyama, T., Walz, J. and Nagayama, K. (1998) Biophys. J. 74, 1409–1420.
[8] Ohno, K., Takeuchi, Y. and Yoshida, M. (1981) Photochem. Photobiol. 33, 573–578.
[9] Hendler, R.W., Dancshazy, Z., Bose, S., Shrager, R.I. and Tokaji, Z. (1994) Biochemistry 33, 4604–4610.
[10] Shrager, R.I., Hendler, R.W. and Bose, S. (1995) Eur. J. Biochem. 229, 589–595.
[11] Tokaji, Z. and Dancshazy, Z. (1997) Biochem. Biophys. Res. Commun. 233, 532–536.
[12] Mukhopadhyay, A.K., Bose, S. and Hendler, R.W. (1994) Biochemistry 33, 10889–10895.
[13] Danshina, S.V., Drachev, L.A., Kaulen, A.D. and Skulachev, V.P. (1992) Photochem. Photobiol. 55, 735–740.
[14] Mostafa, H.I.A. (2004) Biochem. Biophys. Res. Commun. 315, 857–865.
[15] Dracheva, S., Bose, S. and Hendler, R.W. (1996) FEBS Lett. 382, 209–212.
[16] Oesterhelt, D. and Stoeckenius, W. (1974) Methods Enzymol. 31, 667–678.
[17] Schwan, H.P. (1992) Ann. Biomed Eng. 31, 269–288.
[18] Todorov, G., Sokerov, S. and Stoylov, S.P. (1982) Biophys. J. 40, 1–5.
[19] Mostafa, H.I.A., Váró, Gy., Tóth-Boconádi, R., Dér, A. and Keszthelyi, L. (1996) Biophys. J. 70, 468–472.
[20] Mostafa, H.I.A. (1998) Fine structure of the fast electric signal in bacteriorhodopsin, Ph.D. (Candidate of Science) Hungarian Academy of Science.
[21] Cole, K.S. and Cole, R.H. (1941) J.Chem. Phys. 9, 341–351.
[22] Hampp, N. (2000) Chem. Rev. 100, 1755–1776.
[23] Persike, N., Pfeiffer, M., Guckenberger, R. and Fritz, M. (2000) Colloids Surf. B Biointerfaces 19, 325–332.
[24] Lewis, B.A., Rosenblatt, C., Griffin, R.G., Courtemanche, J. and Herzfeld, J. (1985) Biophys. J. 47, 143–150.
[25] Stoeckenius, W., Lozier, R.H. and Bogomolni, R.A. (1979) Biochim. Biophys. Acta. 505, 215–278.
[26] Hendler, R.W. and Bose, S. (2003) Eur. J. Biochem. 270, 3518–3524.
[27] Pedael, A., Daisy, R., Horowitz, M. and Fischer, B. (1998) Optics Lett. 23, 1173–1175.

[28] Korchemskaya, E.Ya., Stepanchikov, D.A. and Dyukova, T.V. (2000) Opt. Mater. 14, 185–191.
[29] Zhang, L., Zeng, T., Cooper, K. and Claus, R.O. (2003) Biophys. J. 84, 2502–2507.
[30] Hanamoto, J.H., Dupuis, P. and El-Sayed, M.A. (1984) Proc. Natl. Acad. Sci. USA. 81, 7083–7087.
[31] Komrakov, A.Y. and Kaulen, A.D. (1994) FEBS Lett. 340, 207–210.
[32] Friedman, N., Ottolenghi, M. and Sheves, M. (2003) Biochemistry 42, 11281–11288.
[33] Schenkl, S., Portuondo, E., Zgrablic, G., Chergui, M., Suske, W., Dolder, M., Landau, E.M. and Haacke, S. (2003) J. Mol. Biol. 329, 711–719.
[34] Porschke, D. (2003) J. Mol. Biol. 331, 667–679.
[35] Joshi, M.K., Dracheva, S., Mukhopadhyay, A.K., Bose, S. and Hendler, R.W. (1998) Biochemistry 37, 14463–14470.
[36] Hauss, T., Buldt, G., Heyn, M.P. and Dencher, N.A. (1994) Proc. Natl. Acad. Sci. USA. 91, 11854–11858.
[37] Xiao, W., Brown, L.S., Needleman, R., Lanyi, J.K. and Shin, Y.-K. (2000) J. Mol. Biol. 304, 715–721.
[38] Rouhani, S., Cartailler, J.P., Facciotti, M.T., Walian, P., Needleman, R., Lanyi, J.K., Glaeser, R.M. and Luecke, H. (2001) J. Mol. Biol. 313, 615–628.
[39] Geibel, S., Friedrich, T., Ormos, P., Wood, P.G., Nagel, G. and Bamberg, E. (2001) Biophys. J. 81, 2059–2068.